IMPROVED INFRASOUND LOCATIONS THROUGH REFINING ATMOSPHERIC MODELS USING WIND DATA AND GROUND-TRUTH INFRASOUND EVENTS

Michael S. O'Brien[1], J. Roger Bowman[1], and Douglas P. Drob[2]

Science Applications International Corporation[1] and Naval Research Laboratory[2]

Sponsored by Army Space and Missile Defense Command

Contract No. W9113M-06-C-0027[1,2]

ABSTRACT

One of the principal functions of infrasound in nuclear-explosion monitoring is to locate low atmospheric and near-surface nuclear explosions in areas that have relatively poor coverage by other sensor technologies (e.g., the southern oceans). This includes regional scenarios for which accurate location is an important discriminant. Recent infrasound studies suggest that the ability to locate events accurately is often limited by erroneous predictions of infrasound observables (arrival time and back azimuth) from which location is estimated, even when advanced atmospheric state specifications are available. A wealth of new atmospheric wind measurements reveals significant inaccuracy in the atmospheric Horizontal Wind Model (HWM-93) and Ground to Space (G2S) wind model between elevations of 60 and 120 km as likely the single largest source of these infrasound prediction errors. To address this problem, we will revise these wind models with a voluminous database of recently available and validated upper atmospheric wind measurements. Our approach will be novel in that we will use the growing number of ground-truth infrasound events in the Space Missile Defense Command (SMDC) Monitoring Research Program databases as atmospheric soundings. These infrasonic ground-truth events will be used to complement the wind measurements in constraining new models, as well as to assess their overall predictive accuracy. We will improve both HWM-93 and G2S but will emphasize the HWM climatological models and corrections because they apply to all locations and times and, thus, will improve our general infrasound event location capability. Here we describe both the atmospheric wind data and infrasound data that will be used to generate and validate new models and subsequent performance in event analysis. We also describe the procedures for data analysis and preparation, the process for assimilating the data into new wind models, and the approach we will employ for assessing the new models.

OBJECTIVES

The primary purpose of this project is to improve our general ability to locate infrasound events by improving the Horizontal Wind Model used in the prediction of infrasound observables using recent wind measurements and direct infrasound observations.

A second purpose of this project is to evaluate statistically, i.e., against a large set of infrasound observations, the ability of the old and new atmospheric models to locate infrasound events and to predict the principal infrasound observables, arrival time and back azimuth.

RESEARCH ACCOMPLISHED

Background

The ability to locate event sources accurately is a central element of nuclear explosion monitoring. In regional scenarios, it can provide important corroboration of explosive events but only if signals can be reliably attributed. Location and, thus, location-related observables are central to source attribution. In remote regions that are not well monitored by other land-based technologies, such as the southern oceans, infrasound may provide the only information that constrains location.

The reliability of infrasound source locations depends on the reliability with which signal features can be predicted from source properties. This requires detailed knowledge of sound propagation in the atmosphere and the physical properties that control it, in particular, the sound speed. The state of the art in representing the atmospheric properties pertinent to infrasound propagation is the Naval Research Laboratory (NRL) Ground to Space (G2S) model (Drob and Picone, 2000; Drob et al., 2003). This model combines climatological data captured in NRL's total atmospheric model (NRLMSISE-00) and HWM-93 with numerical weather prediction (NWP) data such as the Navy Operational Global Atmospheric Prediction System (NOGAPS) and the National Oceanic and Atmospheric Administration (NOAA)-National Center for Environmental Prediction Global Forecast System (NCEP-GFS). The inclusion of the NWP data in G2S significantly improves estimates of tropospheric and stratospheric wind jets that profoundly influence sound speed at lower altitudes (<50 km). Wind models that are based solely on climatology often substantially underestimate tropospheric and stratospheric wind jets, which leads to significant under prediction of the fraction of energy that is ducted through these layers (Drob and Picone, 2000; Drob et al., 2003).

While the G2S models are the most comprehensive atmospheric representation available, significant infrasound residuals are still obtained using them. Le Pichon et al. (2005) found that back-azimuth residuals using G2S models averaged several degrees for repeated thermospheric propagation paths. O'Brien and Shields (2004) compared G2S predictions to observations from 21 ground-truth (GT) events at different locations. They assumed that one could unambiguously identify the duct in which a signal propagated but not the specific path traveled, as when one does not know the location of a source. So, they compared observations to model predictions averaged over each duct. They found that the additional ambiguity raised travel-time and back-azimuth residuals to almost 10% and 7°, as illustrated in the histograms of Figure 1.

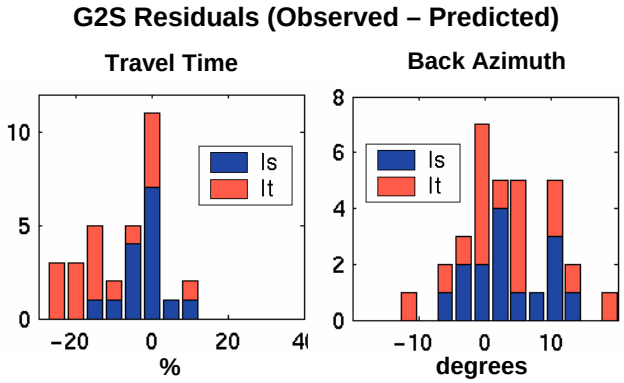

Figure 1. Residuals between infrasound observations and G2S model predictions indicate typical discrepancies of 10% in travel time and 7º in back azimuth.

The principal source of these discrepancies appears to be the wind model in the mesospheric / lower thermospheric (MLT) region where weather data cannot assist. Recent direct measurements of winds at higher elevations indicate that HWM-93 significantly underestimates winds there. This is illustrated by the two independent sets of optical satellite-based wind measurements in Figure 2, which consistently and substantially exceed the HWM-93 predictions, at times by up to 65 m/s. Similar wind corrections were also obtained by Le Pichon et al. (2005) who used the infrasound residuals to constrain the MLT region winds.

In this project, we use the extensive measurements of MLT winds made since HWM-93 and GT infrasound observations to improve the wind model, thereby improving our infrasound prediction capability. Our goal is to create two new HWMs: one constrained only by the new set of atmospheric data, the other constrained by atmospheric and infrasound data. We will also derive corresponding G2S models from the new HWMs.

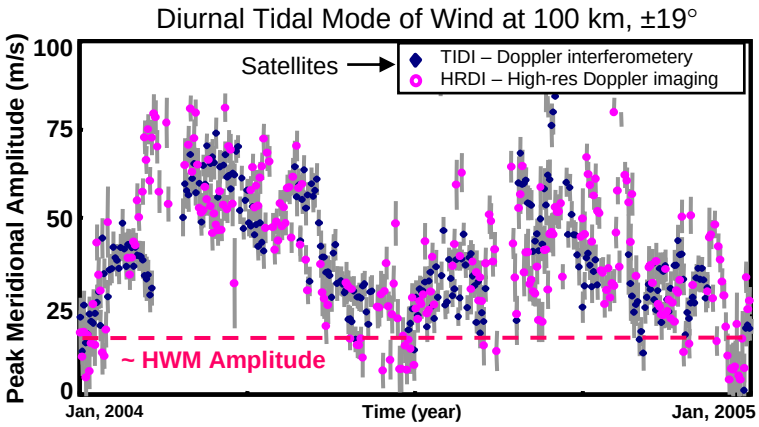

Figure 2. Meridional winds associated with the diurnal tidal mode at an elevation of 100 km measured globally between ±19°. Wind measurements made since HWM-93 was created (Hedin et al., 1996; Picone et al., 2002) disagree with the model predictions consistently and substantially, at times by as much as 65 m/s.

To generate and vet these models we will follow an iterative process along two tracks as illustrated in Figure 3 below. On one track, we will prepare atmospheric data and use them to generate and refine atmospheric wind models. On the second track, we will assemble an event data set, derived largely from events and waveforms already available in the SMDC Monitoring Research Program's Infrasound Database (IDB) and waveform archives and then analyze signals to measure arrival time, back azimuth, slowness, amplitude, etc. The two tracks converge when we evaluate models by comparing predictions from the atmospheric models with the measured observables. The results of the evaluation will then be used to refine our understanding of propagation paths analyzed signals. The components of this process and progress are described in the following subsections.

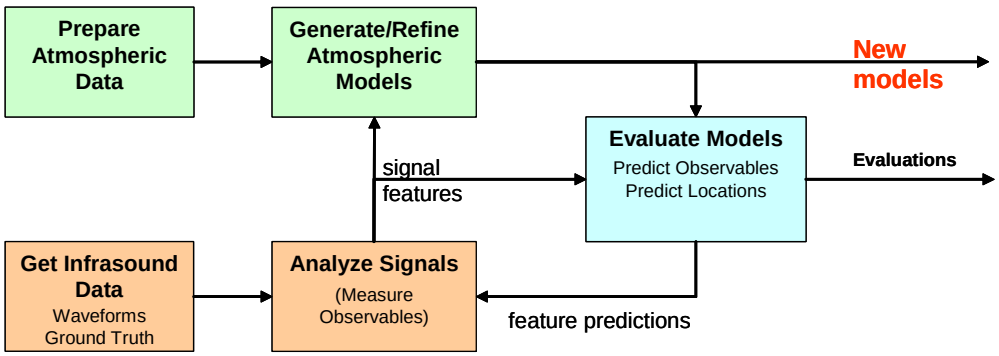

Figure 3. Process for refining atmospheric wind models using wind and infrasound data. The process iteratively refines the atmospheric models as the data sets are expanded and refined and the inversion methodology is developed.

Atmospheric Data

The NRL has been collecting and validating atmospheric data for the past ten years. The current NRL database represents more than 30 times the number of individual atmospheric observations than available when HWM-93 was created. More importantly, the new observations fill a number of critical gaps in the spatiotemporal distribution of the previous database, particularly in the 90 to 120 km region. A partial list of the recent satellite and ground-based data sets that have been assembled at NRL and that we will bring to bear is shown in Table 1. The details on each of these data sets are beyond the scope of this paper. All of these data sets have been well vetted and validated in the open scientific literature (Drob et al., 2000; Swinbank and Ortland, 2003; Larsen et al., 2003) and are available for use. However, these data must be carefully selected, partitioned, and weighted to ensure that the number of data points is distributed as evenly as possible over the represented ranges of altitude, latitude, local time, day-of-year, etc., before application of the parameter estimation process.

Table 1. Atmospheric wind measurements made available since HWM-93 was developed.

Data Type	Experiment	Years	Altitude (km)	Location	Local Time Coverage	Field
NWP Synthesis	NCEP/GFS, GEOS4, ...	93 – now	0 – 60	Global	4x daily	T, U, V
NASA/UARS (satellite)	HRDI (Level 2B)	92 – 98, 05	50 – 110	± 60º	Day/Night	T, U, V
	WINDII	92 – 98	80 – 300	± 70º	Day/Night	T, U, V
	HALOE	92 – 98	35 – 90	± 70º	Twilight	T
NASA/TIMED (satellite)	TIDI	00 – now	60 – 110	± 85º	Day/Night	U, V
	SABER	00 – now	35 – 95	± 85º	Day	T
LIDAR	Colorado State (Na)	93 – now	80 – 105	41 N, 103 W	Night	T, U, V
	Urbana (Na)	96 – 98	80 – 105	40 N, 88 W	Night/Day	T, U, V
	Bear Lake (Rayleigh)	94 – 96	30 – 80	41 N, 111 W	Night	T
	Urbana (Rayleigh)	95 – 96	30 – 80	40 N, 88 W	Night	T
MF RADAR	Christmas Island, Kiribati	92 – 93	70 – 96	2 N, 157 W	Continuous	U, V
	Bribe Island, Australia	95	70 – 96	28 S, 153 N		
	Adelaide, Australia	01 – 04	70 – 98	34 S, 138 E		
	Davis, Antarctica	01 – 04	50 – 100	68 S, 77 E		
	Poker Flat, Alaska	98 – 04	44 – 108	65 N, 147 W		
	Yamagawa, Japan	98 – 03	60 – 98	31 N, 130 E		
	Wakkanai, Japan	97 - 03	60 – 108	45 N, 141 E		
	Titunelveli, India	01 – 02	68 – 98	8 N, 77 E		
ISR RADAR	Arecibo, Puerto Rico	83 – 99	100 – 170	18 N, 67 W	Day	V
	Millstone Hill, Mass.	88 – 99	105 – 135	43 N, 72 W		
	Sondrestrom, Greenland	87 – 91	105 – 135	67 N, 147 W		
Rocket	TMA chemical trails	58 – 02	85 – 150	Sparse/Global	Day/Night	U, V
	Falling sphere	58 – 02	75 – 110	Sparse/Global	Day/Night	T

Generation of Horizontal Wind Models

The NRL data assimilation process is illustrated in Figure 4. In HWM-93 vertical, horizontal, and temporal variations are represented with associated Legendre polynomials, polynomials, and Fourier harmonics, respectively (Hedin et al., 1996). Its approximately 1000 model coefficients were computed using a subset of only 9000 data points (from a much larger population of measurements from over 20 different instruments) because of the computational limitations at the time. This limited spatiotemporal coverage meant that higher order spectral terms could not be resolved, so the model resolution was effectively limited to a relatively low order (harmonic degree and order six). Subsequent advances in computing, and the availability of new data sets, mean that we can now fuse 100 times the number of data into a new HWM. This will dramatically improve HWM resolution and accuracy, and thus infrasound predictions.

Our HWM/MSIS data assimilation routines are based on Levenberg-Marquardt fitting (Press et al., 1994) extended by modification of the convergence parameter trust region. Subsets of parameters are matched with constraining data (i.e., geographically and temporally nearby) and fitted to those data individually to increase efficiency and stability. The ability to specify limiting constraints is provided through the method of target values. The fitting process iterates until the chi-squared for each parameter subset changes less than 0.1%. Statistical diagnostics allow us to assess the quality of the fit by analyzing the influence of different data on different parameters, data cross correlations, etc.

The data assimilation process accommodates multiple, diverse datasets of varying space-time densities to achieve the most comprehensive coverage. We will explicitly address the issues of statistical independence and data quality within each data subset. This is important for ensuring that the small set of high quality infrasound observations is not overwhelmed by the comparatively vast but statistically dependent (i.e., repetitive) sets of atmospheric data. We pre-balance the content of independent information among the data that go into the fitting process through a combination of subsampling and error-weighted averaging over evenly spaced bins in space-time. We also

determine optimal observational error scaling or weighting factors (σ_i) for each dataset by instrument and wind component. This will allow us to let the infrasound observations control the parameter estimation process, whether for reasons of higher data quality or relative statistical independence, of those model parameters for which information is provided.

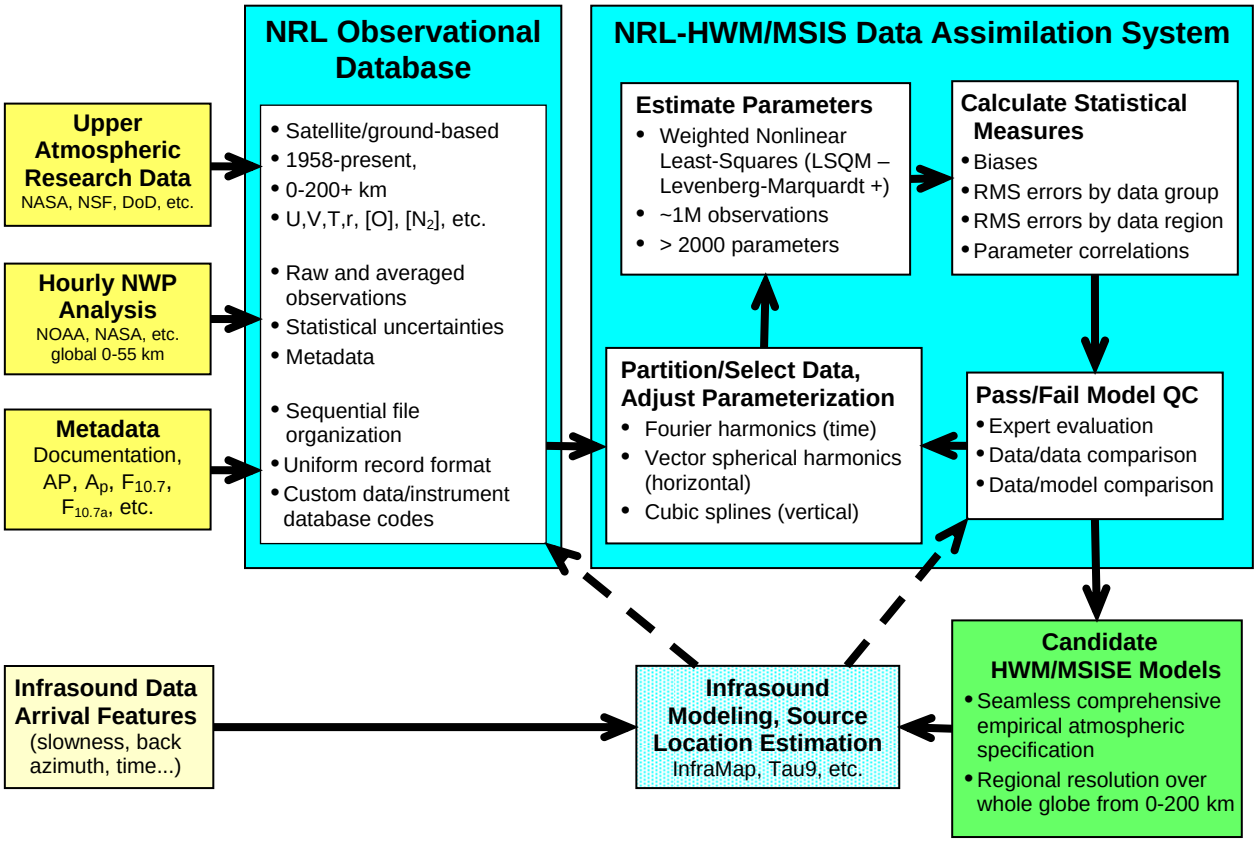

Figure 4. Process for assimilation of wind and infrasound data into new HWM models.

Infrasound Ground-Truth Events

Given the extensive space-time complexity of the atmospheric winds, we seek as many infrasound observations as possible with which to constrain or validate models. We have begun the collection of our GT data set for validating and constraining existing and new models by building on SMDC's existing IDB, which contains events from a variety of source types spanning several decades. We consider here a superset of the IDB, augmented with recent events. We will continue to augment our data set as events are identified and data become available. Figure 5 illustrates the global distribution of 264 events currently in the set.

However, prediction residuals, specifically in the travel time T (the difference between arrival and source times) and back azimuth deflection A (the difference between arrival and source-receiver back azimuths) are partly the result of errors in measured arrival properties, time t and back azimuth a, and GT source parameters, time τ, location r, and elevation e. Many events in our data set will have little utility for model constraint or assessment because the measurement- and ground-truth-related errors are too large compared to the model-related errors – from the background discussion, that will start to be the case when the errors are more than a few percent in T or a few degrees in A. We can estimate the fractional uncertainty σ_T in T and the total uncertainty σ_A in A in terms of the arrival measurement uncertainties σ_t and σ_a in t and a, and the source parameter uncertainties σ_τ, σ_r and σ_e in τ, r, and e. Letting R represent source-receiver range and $V=R/T$ the group velocity:

$$\sigma_T^2 \approx \left(\sigma_t^2 + \sigma_r^2/V^2 + \sigma_e^2/V^2 + \sigma_\tau^2\right)/T^2$$
$$\approx \sigma_t^2 V^2/R^2 + \sigma_r^2/R^2 + \sigma_e^2/R^2 + \sigma_\tau^2 V^2/R^2 \quad (1)$$

$$\sigma_A^2 \approx \sigma_a^2 + \sigma_r^2/R^2 \quad (2)$$

Note that the source-related parts of both errors are range dependent. Thus, we cannot assess the constraining value of data on an event basis, even if we assign measurement errors σ_a and σ_t uniformly – we must do so signal by signal. Since the effects of the errors diminish with range, it is possible for less well-characterized sources to constrain the wind models if observed at long enough range. Note also that travel times contain more source-related errors than back-azimuth deviation, so in general, arrival-time data will be less useful than back-azimuth data.

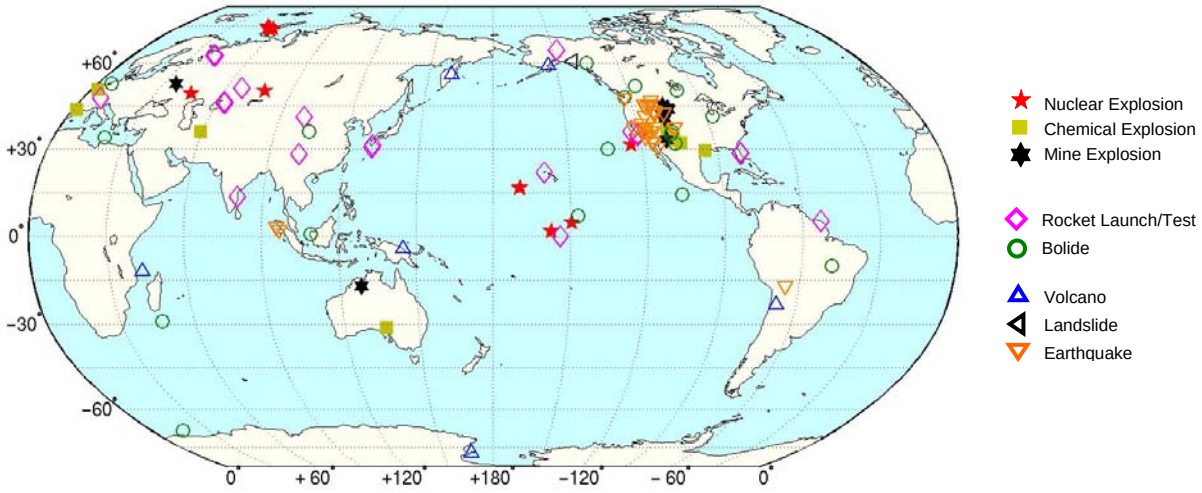

Figure 5. The distribution of sources in the expanded data set.

Equations 1 and 2 ultimately make their way into the significance statistics in the next section, as a continuous mechanism for weighting data in proportion to their constraining power. However, we can make a preliminary assessment of which event data have enough accuracy to be worth considering at all, by assigning values to the source errors σ_τ, σ_r and σ_e for each event and setting liberal upper thresholds on σ_A and σ_T for rejecting the arrival data outright. Figure 6 illustrates the travel paths for the remaining signals in the data set where either threshold $\sigma_T < 3\%$ and $\sigma_A < 3°$ was passed for our preliminary assignment of source errors discussed next. We neglect arrival property errors σ_a and σ_t to focus only on the effects of source parameter errors. For the purpose of display, we have used colors to represent the number of paths whose endpoints fall within the same pair of 1° bins.

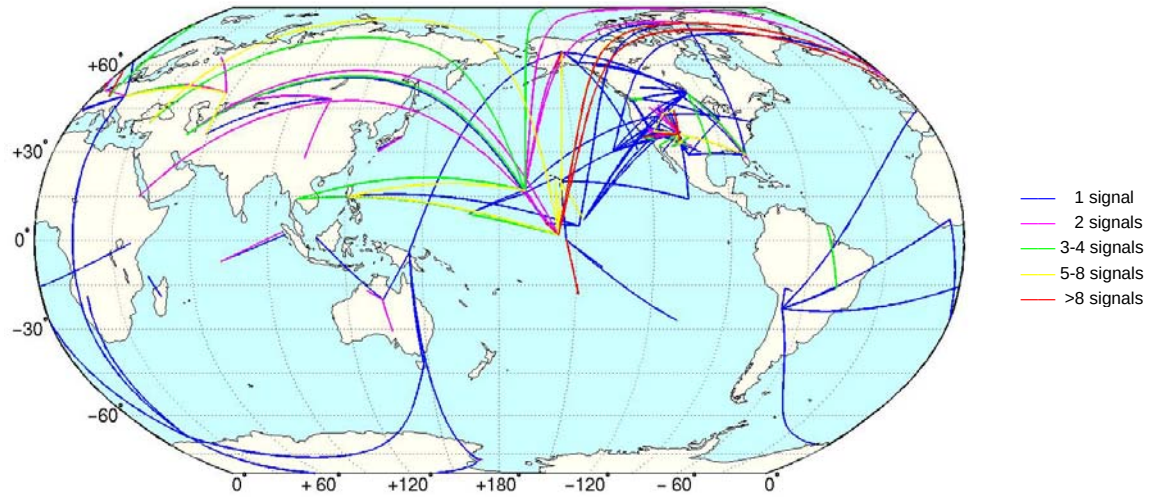

Figure 6. The distribution of signal paths for which source-related errors are $\sigma_T < 3\%$ and $\sigma_A < 3°$.

The accuracy assessment depends strongly on the assignment of source uncertainties, a laborious undertaking that often requires significant detective work. Three broad categories of events fall out of the related considerations. The rough distribution of events among them is summarized in Table 2. The first category is composed of well-known, impulsive, stationary events – mostly nuclear explosions (e.g., Operation Dominic, 1961) and controlled chemical explosions (e.g., Watusi, 2003; White Sands Missile Range Infrasound Calibration Experiments, 2005, 2006), and some mining explosions, where source location and time were independently measured and recorded. Source parameters for these events are generally constrained well enough that their contributions to σ_A and σ_T are much smaller than those from the models or the arrival measurements. For this group of events we set σ_r,σ_e, and σ_τ to half the least significant digit of officially stated source parameters where we believe precision is reflective of accuracy (generally the case), although we set floors of σ_r,σ_e=1 m on location and σ_τ=1 s on time.

The second category is the much broader collection of partially constrained sources for which errors must be evaluated on a case-by-case basis. Locations for many accidental explosions can be determined precisely after the fact. However, the best time constraints come from eyewitness accounts, post-accident reports, etc., which are often of poor or marginal quality. For these events we conservatively set σ_τ to a minimum of 120 s, even in cases where time was specified to the minute. For earthquakes and mining explosions whose locations are estimated seismically we uniformly set σ_r=20 km, σ_τ=10 s and σ_e=0 km; case-specific assessments will be made in the future. Volcanic eruptions are generally well located so we set σ_r=0.5 km. For isolated explosive eruptions we set σ_τ=60–600 s depending on available accounts. We have not yet added continuous eruption data such as those from Vanuatu observed at station I22FR (Le Pichon et al., 2005). For these event sequences, energy cannot be matched up one-to-one with specifically timed sources, so we will likely set σ_τ large, essentially discarding time data.

Table 2. Distribution of event sources and qualities.

Event Source Type	1	2	3
Nuclear test explosion	31	22	
Chemical explosion	14	7	
Mine explosion		40	
Rocket launch/re-entry/test	1		77
Bolide			21
Volcano/Earthquake		51	
Total	**46**	**120**	**98**

1 – Well constrained, impulsive, stationary
2 – Partially constrained, stationary, possibly non-impulsive
3 – Moving

Events in the third category have moving sources: rocket launches, re-entries, and bolides. This may be a controversial set of events because it is difficult to constrain the space-time-amplitude function of the objects as infrasound sources. On the other hand, it is a potentially important set because bolides and rocket launches are frequent compared to controlled, stationary sources of appreciable size. Bolides typically traverse the atmosphere in several seconds, traveling tens to hundreds of kilometers laterally and release significant energy as they disintegrate, sometimes explosively. While their source durations are brief, their exact times are often known only through eyewitness accounts. In such cases we have assigned large source errors σ_τ =60–120 s, σ_r =100 km, σ_e =5–20 km, depending on the quality of accounts, which eliminates most of their data against any reasonable thresholds on σ_A and σ_T. However, optical satellite imagery has fixed the precise time and location of detonation of some bolides, which we have equated to the predominant time and location of infrasound production and assigned σ_t as low as 2–5 s, and σ_r and σ_e as low as 1 km.

In contrast, rocket launches take minutes to exit the atmosphere while traveling hundreds of kilometers laterally. Where only launch time and location constrain the source, we have respectively assigned σ_τ =120 s, σ_r =100 km and σ_e=30 km, effectively eliminating all of their data. However, as with bolides, there are theoretically favorable points along the path for the rockets to generate infrasound, such as sonic/supersonic transition points. Impulsive signals, such as those for Delta 289 or Delta 290 in Figure 7(a) serve as evidence that this is the case. Approximate trajectories can be constructed for some rocket launches, (e.g., Gibson and Norris, 2002, 2004b) allowing these points to be more closely located. Profiles for three launches from Vandenberg AFB detected at I57US are illustrated in Figure 7(b). Trajectory information also allows sources to be modeled as lines, as Arrowsmith et al. (2003) did for the Washington state fireball. Then arrival features can be compared as whole sets to predictions, thereby providing not only the properties of individual arrivals as validation data, but also their progressions with time and values relative to one another. In these cases we have been more optimistic, setting σ_t =30 s, σ_r =5 km and σ_e ~5 km.

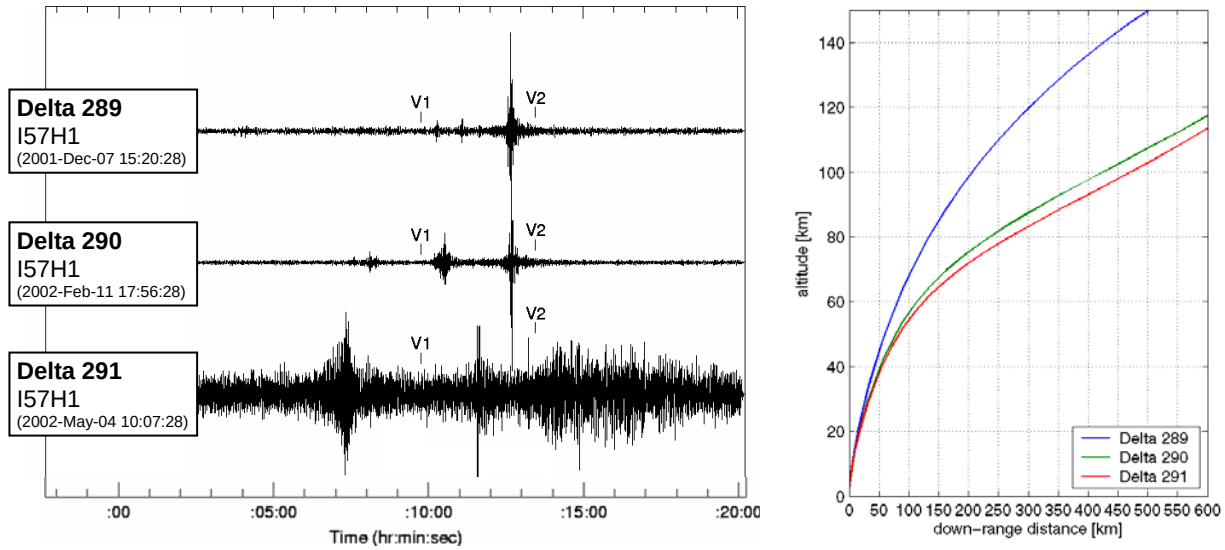

(a) (b)

Figure 7. (a) Infrasound traces at I57US from three rocket launches from Vandenberg AFB and (b) corresponding flight profiles constructed from launch parameters.

For the 632 signals currently in the expanded IDB data set, about half of the arrival-time data and a third of the back-azimuth data failed to pass the preliminary winnowing thresholds of $\sigma_T < 3\%$ and $\sigma_A < 3°$. However, this set will change, perhaps substantially, as knowledge of source parameters and our uncertainties in them is improved, as the IDB is expanded with new events and data, and as signal properties are measured and their accuracies systematically assessed.

Infrasound Validation of Wind Models

For the purposes of nuclear explosion monitoring, the new wind models must be evaluated in terms of accuracy with which they make infrasound predictions. Given the highly variable nature of the atmosphere and the dramatic effects that the variability has on infrasound propagation, it can be difficult to assess how one model improves prediction over another, so a statistical approach is essential. We follow the approach of O'Brien and Shields (2004) by formulating statistical hypothesis tests from the residuals between GT data and the predictions of each model.

Where possible, we evaluate the location accuracy associated with a given atmospheric model by directly comparing the source locations and times it predicts from arrival measurements to GT values. Generally, this is a multiple arrival problem, since a single arrival cannot uniquely specify the four space-time source coordinates, even if all of arrival time, back azimuth and slowness are usable data. However, the formulation of tractable statistics for multiple arrivals is dependent on the particular way in which data are combined with one another. Here we consider an alternative approach, in which we specify the least variable of the source parameters, elevation, and define measures of fit for the other three that sum over the predictions from all the arrivals. From those, we create statistics with approximate F distributions with which to test the significance of the differences between predictions of pairs of models. The residuals Δ, sample measures of fit s^2, and significance statistics F are listed below, where along- and cross-path location error components are denoted by $\|$ and $\perp$, the number of arrivals by N, and wind models by i and j. As above, uncertainty is denoted by σ, source location and time by r and τ, arrival time and back azimuth by t and a, and travel time by T. Following O'Brien and Shields (2004), we normalize travel-time residuals by the observed travel time (measured arrival time less the GT source time) and location residuals by the source-receiver range. This removes the expected dependence of the model-related errors, hence the residuals, on source-receiver range. After normalization, the residuals have roughly the same expected size and distribution so they can be combined to form statistics s^2 that are approximately distributed as χ^2, and statistics F that are approximately distributed as F.

Residuals		*Measure of Fit*		*Significance Test Statistic*	
$\Delta_{\tau k} = \frac{(\tau_{pred} - \tau)_k}{(t_{obs} - \tau)_k}$	$\Rightarrow$	$s_\tau^2 = \frac{1}{N-1}\sum_{k=1}^{N}\frac{\Delta_{\tau k}^2}{\sigma_{Tk}^2}$	$\Rightarrow$	$F_{\tau ij} = \frac{s_{\tau i}^2}{s_{\tau j}^2} \sim \mathrm{F}_{N,N}$	(3)
$\Delta_{\|k} = \frac{(r_{pred} - r)_{\|k}}{\lvert \mathbf{r}_{sta} - \mathbf{r}_k \rvert}$	$\Rightarrow$	$s_\|^2 = \frac{1}{N-1}\sum_{k=1}^{N}\frac{\Delta_{\|k}^2}{\sigma_{rk}^2}$	$\Rightarrow$	$F_{\|ij} = \frac{s_{\|i}^2}{s_{\|j}^2} \sim \mathrm{F}_{N,N}$	(4)
$\Delta_{\perp k} = \frac{(r_{pred} - r)_{\perp k}}{\lvert \mathbf{r}_{sta} - \mathbf{r}_k \rvert_k}$	$\Rightarrow$	$s_\perp^2 = \frac{1}{N-1}\sum_{k=1}^{N}\frac{\Delta_{\perp k}^2}{\sigma_{rk}^2}$	$\Rightarrow$	$F_{\perp ij} = \frac{s_{\perp i}^2}{s_{\perp j}^2} \sim \mathrm{F}_{N,N}$	(5)
			$\Rightarrow$	$F_{rij} = \frac{s_{\|i}^2 + s_{\perp i}^2}{s_{\|j}^2 + s_{\perp j}^2} \sim \mathrm{F}_{2N,2N}$	(6)

However, not all of the arrival measurements, time, back azimuth, and slowness are always available or used for estimating location. Often, slowness is disregarded altogether because it provides only weak constraint on the source-receiver geometry; in single detection scenarios, which is often the case for small local or regional events. That leaves only arrival time and back azimuth as reliable data. In some multiple station scenarios, arrival times are dropped also, in favor of back azimuth data because the effects of error in source parameters and assumed propagation path are more pronounced in travel time than back azimuth deflection. Thus, to exploit all GT infrasound observations fully, we must also be able formulate an evaluation in terms of the observables themselves.

Again, following O'Brien and Shields (2004), we formulate measures of fit and model comparison statistics for travel time and back azimuth deflection residuals, *T* and *A*. Note that these are numerically equivalent to residuals in arrival time and back azimuth. Travel-time residuals are normalized as described above. Back azimuth deflection residuals are not, since the model-related back-azimuth errors lack the same systematic dependence on source-receiver range. These statistics allow all arrival time and back-azimuth data to participate in model assessment, whether or not they can be combined into actual location estimates.

Residuals		*Measure of Fit*		*Significance Test Statistic*	
$\Delta_{Tk} = \frac{(T_{pred} - T_{obs})_k}{(T_{obs})_k}$	$\Rightarrow$	$s_T^2 = \frac{1}{N-1}\sum_{k=1}^{N}\frac{\Delta_{Tk}^2}{\sigma_{Tk}^2}$	$\Rightarrow$	$F_{Tij} = \frac{s_{Ti}^2}{s_{Tj}^2} \sim \mathrm{F}_{N,N}$	(7)
$\Delta_{Ak} = (A_{pred} - A_{obs})_k$	$\Rightarrow$	$s_A^2 = \frac{1}{N-1}\sum_{k=1}^{N}\frac{\Delta_{Ak}^2}{\sigma_{Ak}^2}$	$\Rightarrow$	$F_{Aij} = \frac{s_{Ai}^2}{s_{Aj}^2} \sim \mathrm{F}_{N,N}$	(8)
			$\Rightarrow$	$F_{ij} = \frac{s_{Ti}^2 + s_{Ai}^2}{s_{Tj}^2 + s_{Aj}^2} \sim \mathrm{F}_{2N,2N}$	(9)

Once we have defined the final evaluation data set, we will make corresponding predictions using each wind model, and evaluate the measures of fit. We will then evaluate the comparison statistics for each relevant model pair and determine the significance level at which each model is statistically better than the other.

CONCLUSIONS AND RECOMMENDATIONS

We have begun preparation of data for incorporation into new wind models that should dramatically improve infrasound prediction for paths that sample the mesosphere and thermosphere. This includes vast new set of atmospheric wind data, collected mostly by satellite, and warehoused by NRL since the time that HWM-93 was created. This data set, along with infrasound data, indicate that a dramatic improvement in the parameterization of mesospheric and lower thermospheric winds will be possible.

We have also begun the preparation of many infrasound observations for validating the new wind models, building on the existing SMDC infrasound event database. We have defined statistics that will allow for the limited

infrasound data to be maximally exploited to constrain and evaluate the predictive capabilities of new and existing atmospheric models. We estimate that as many as two-thirds of these will yield data that can constrain the new wind models. However, this set is not large. Thus, we recommend that continued efforts to acquire and refine our understanding of GT infrasound so that the set of useful data is expanded, improving our understanding of the winds and the accuracy of wind models we have created.

REFERENCES

Drob, D. P., J. M. Picone, and S. D. Eckerman, C. Y. She, J. F. Kafkalidis, D. A. Ortland, R. J. Niciejewski, and T. L. Killeen (2000). Mid-latitude temperatures at 87 km: Results from multi-instrument Fourier analysis, *Geophys. Res. Lett*. 27: (14), 2109-2112, 10.1029/1999GL010821.

Drob, D.P., J. M. Picone, and M. Garces (2003). Global morphology of infrasound propagation, *J. Geophys. Res*., 108 (D21), 4680, 10.1029/2002JD003307.

Drob D.P., and J.M. Picone (2000). Statistical performance measures of the HWM-93 and MSISE-90 empirical atmospheric models and the relation to infrasonic CTBT monitoring, in *Proceedings of the 22nd Seismic Research Symposium: Planning for Verification of and Compliance with The Comprehensive Nuclear-Test-Ban Treaty*, Vol. 3, pp. 161–169.

Gibson, R. and D. Norris (2002). Integration of near-real-time atmospheric models with InfraMAP and applications to modeling infrasound from rockets, *Proceedings of the 24th Seismic Research Review– Nuclear Explosion Monitoring: Innovation and Integration*, LA-UR-02-5048, Vol.2, 775–782

Gibson, R. and D. Norris (2004b). Integration of InfraMAP software with near-real-time atmospheric characterizations, BBN Technical Report DTRA01-01-C-0084.

Hedin, A.E. (1991). Extension of the MSIS thermosphere model into the middle and lower atmosphere, *J. Geophys. Res*. 96: (A2), 1159–1172, 10.1029/90JA02125.

Hedin, A. E, E. L. Fleming, A. H. Manson, F. J. Schmidlin, S. K. Avery, R. R. Clark, S. J. Franke, G. J. Fraser, T. Tsuda, F. Vial, and R.A. Vincent (1996). Empirical wind model for the upper, middle, and lower atmosphere, *J. Atmos. Terr. Phys*. 58: 1421-1447.

Larsen M. F., A. Z. Liu, R. L. Bishop, and J. H. Hecht (2003). TOMEX: A comparison of lidar and sounding rocket chemical tracer wind measurements, *Geophys. Res. Lett*. 30: (7), 1375, doi:10.1029/2002GL015678.

Le Pichon, A., E. Blanc, D. P. Drob, S. Lambotte, J. X. Dessa, M. Lardy, P. Bani, and S. Vergniolle (2005). Infrasound monitoring of volcanoes to probe high-altitude winds, *J. Geophys. Res*. 110: D13106, 10.1029/2004JD005587.

O'Brien, M. and G. Shields (2004). Infrasound source locations using time-varying atmospheric models, in *Proceedings of the 26th Seismic Research Review: Trends in Nuclear Explosion Monitoring*, LA-UR-04-5801, Vol. 2, 660–669.

Picone, J. M., A. E. Hedin, D. P. Drob, and A. C. Aikin (2002). NRLMSISE-00 empirical model of the atmosphere: Statistical comparisons and scientific issues, *J. Geophys. Res*. 107: (A12), 1468, 10.1029/2002JA009430.

Press, W. H., B. P. Flannery, S. A. Teukolsky, and W. T. Vetterling (1994). Numerical recipes: the art of scientific computing, Cambridge University Press, New York.

Swinbank R. and Ortland D. A. (2003). Compilation of wind data for the Upper Atmosphere Research Satellite (UARS) Reference Atmosphere Project, *J. Geophys. Res*. 108: (D19), 4615, 10.1029/2002JD003135.